

Influence of Different Percentages of Copper on the Size and Optical Properties of Ag-Cu Nanoparticles Formed by Wet-Chemical Method

P. Mashayekhshams^{a,*} and A. Banaei^b

^aDepartment of chemistry, Science and Research branch, Islamic Azad university, Tehran, Iran

^bDepartment of chemistry, Payame Noor university, Tehran, Iran

(Received 30 March 2015, Accepted 1 October 2015)

In this work, Ag-Cu nanoparticles (with different percentages of copper, 10%, 25%, 50%, 75% Cu) were synthesized by wet chemical method. Copper(II) sulfate and silver nitrate were taken as metal precursors, ascorbic acid as reducing agent and anhydride maleic (MA) as a modifier. The prepared nanoparticles were characterized by means of X-ray diffraction (XRD) technique and scanning electron microscopy (SEM-EDAX), Fourier transform infrared spectroscopy (FT-IR) and UV-Vis spectroscopy. SEM indicated the formation of uniform spherical crystalline nanoparticle in a well distributed size and morphology. It can be seen from these pictures that the particle size decreased with increasing of the copper percent. When the molar ratio of $\text{Cu}^{2+}/\text{Ag}^+$ is 75/25 (>50%), mixture of the spherical and hexagonal nanoparticles was prepared. Three pronounced Ag diffraction peaks (111), (200) and (220) appeared at $2\theta = 38^\circ$, 43.9° and 64.1° , respectively. The three most intense peaks of the XRD pattern of sample showed a slight shifting of the center of the diffraction peaks toward a lower angle. No shifting was observed in XRD lines with the increase of Cu^{2+} to Ag^+ ratio in the $\text{Cu}^{2+}/\text{Ag}^+$ mixed solution (> 50% Cu). Fourier transform infrared spectroscopy (FT-IR) showed that nanoparticles are coordination between oxygen atoms and nanoparticles, because functional unit C=O present in MA, shifts to 1652.69 cm^{-1} after embedding nanoparticles. The position of the surface plasmon resonance (SPR) absorption band on the nanoparticles could be shifted from 380-350 nm *via* the change of their percentage of Cu.

Keywords: Different percentages of copper, Control size, Copper-silver, Wet-chemical method, Optical properties

INTRODUCTION

Bimetallic nanoparticles have unique optical, magnetic, and catalytic properties, which are very different from those of their monometallic nanoparticles [1]. For this reason, they have received considerable attention recently for the expansion of new synthesis methods for bimetallic nanoparticles. The most important examples of bimetallic nanoparticles are Ag-Au, Ag-Cu, Au-Cu and Au-pd [2]. Optical properties of metal nanoparticles have caught much interest recently [3]. As optical properties are dependent on the frequency at which the surface plasmon resonance (SPR) occurs, the ability to improve the SPR frequency is of great importance [4]. The SPR frequency of a metal particle

depends on the particle size, particle morphology, structure, composition [5] and can be changed by the incorporation of another metal element in it. Here, we synthesized Ag-Cu (10%, 25%, 50%, 75%) nanoparticles by wet-chemical method, and then, studied the size, size distribution, crystal structure and optical properties of bimetallic Ag-Cu nanoparticles with different percentages of copper. Finally, by controlling the initial percentages of copper and silver ions in the reaction mixtures, we controlled the size, distribution size, and SPR frequency of Ag-Cu nanoparticles.

EXPERIMENTAL

Materials

All of the reagents were used as purchased without

*Corresponding author. E-mail: pr Mashayekhi@gmail.com

further purification. Copper(II) sulfate pentahydrate salt ($\text{CuSO}_4 \cdot 5\text{H}_2\text{O}$) of 98% purity (Merck), and silver nitrate (AgNO_3) (Merck), were dissolved in de-ionized water. Anhydride maleic ($\text{C}_4\text{H}_2\text{O}_3$), ascorbic acid ($\text{C}_6\text{H}_6\text{O}_6$), were purchased from Sigma-Aldrich.

Method

Synthesis of Cu-Ag nanoparticles started with dissolving anhydride maleic (0.001 M) in deionized water. Next, silver nitrate (0.1 M) and copper(II) sulfate (0.00755 M, 0.022 M, 0.06 M and 0.204 M) were dissolved in deionized water, and then were added to the aqueous solution containing the modifier in flask, while vigorously stirring. Into this mixture, mixture ascorbic acid (0.04 M) and sodium hydroxide (0.2 M) were rapidly injected with constant stirring and under N_2 atmosphere. Color change occurred in the aqueous phase to black. When the solution color did not change, the reaction was ceased [6]. The synthesized nanoparticles were centrifuged (12000 rpm, 20 min), and then washed 3-4 times by de-ionized water and 2-3 times with ethanol. The powder of Ag-Cu nanoparticles was characterized by scanning electron microscopy (SEM) and X-ray diffraction (XRD) and UV-Vis spectroscopy. Instrument D5000-Siemens XRD with graphite monochromatized Cu $K\alpha$ radiation ($\lambda = 1.541 \text{ \AA}$) was used for recording X-ray diffraction (XRD) pattern operating at 30 kV operation voltage and 40 mA current in the 2θ range of 20° - 80° . Scanning electron microscopy (SEM) images was conducted using a LEO 1430 VP microscopy. UV-Vis spectra were measured on Shimadzu UV-1601PC spectrophotometer. Infrared (IR) spectrum was measured on a Perkin Elmer RXI fourier transform infrared (FTIR) spectrometer.

RESULTS AND DISCUSSION

SEM Characterization

The morphology of the Ag-Cu nanoparticles was studied with SEM. The spherical particles are seen from the SEM micrographs. The Cu-Ag nanoparticles exhibit uniform shape. It can be seen from these pictures that the particle size is decreased with the increase of copper percentage. When the molar ratio of $\text{Cu}^{2+}/\text{Ag}^+$ was 75/25 (>50%), mixture of the spherical and hexagonal nanoparticles was

prepared.

EDAX analysis was done to recognize the elemental composition of the synthesized nanoparticles. Figure 2 shows EDAX spectrum of Ag-Cu nanoparticles (for 50% Cu) that Ag is major element; 10% Cu and 87% Ag.

XRD Diffraction Analyses

Figure 3 shows the XRD pattern of Ag-Cu nanoparticle. All the diffraction peaks can be well indexed to face-centered cubic (FCC) Ag, Cu according to the JCPDS cards (NO.1-1167) and (NO.4-836). Three pronounced Ag diffraction peaks (111), (200) and (220) appeared at $2\theta = 38^\circ$, 43.9° and 64.1° , respectively. The three most intense peaks of the XRD pattern of the sample showed a slight shifting of the center of the diffraction peaks toward a lower angle. No shifting was observed in XRD lines with the increase in the ratio of Cu^{2+} to Ag^+ in the $\text{Cu}^{2+}/\text{Ag}^+$ mixed solution (> 50% Cu). The size of the samples was calculated from the debye-scherer formula using (111) reflection on XRD pattern.

Peak Ag (111) for 50% Cu:

$$\beta = (38.64 - 37.2) \times \frac{3.14}{180} = 0.0250 \text{ radians}$$

$$2\theta = 38 \rightarrow \theta = 19$$

$$D = \frac{0.9\lambda}{\beta \cos \theta} \rightarrow D = \frac{0.9 \times 0.154}{0.0250 \times \cos 19} = 5.9 \text{ nm}$$

Peak Ag (111) for 25% Cu:

$$\beta = (38.2 - 37) \times \frac{3.14}{180} = 0.020 \text{ radians}$$

$$2\theta = 37.8 \rightarrow \theta = 18.9$$

$$D = \frac{0.9\lambda}{\beta \cos \theta} \rightarrow D = \frac{0.9 \times 0.154}{0.020 \times \cos 18.9} = 7.3 \text{ nm}$$

Peak Ag (111) for 10% Cu:

$$\beta = (37.7 - 36.9) \times \frac{3.14}{180} = 0.0139 \text{ radians}$$

$$2\theta = 37.2 \rightarrow \theta = 18.6$$

$$D = \frac{0.9\lambda}{\beta \cos \theta} \rightarrow D = \frac{0.9 \times 0.154}{0.0139 \times \cos 18.6} = 10.5 \text{ nm}$$

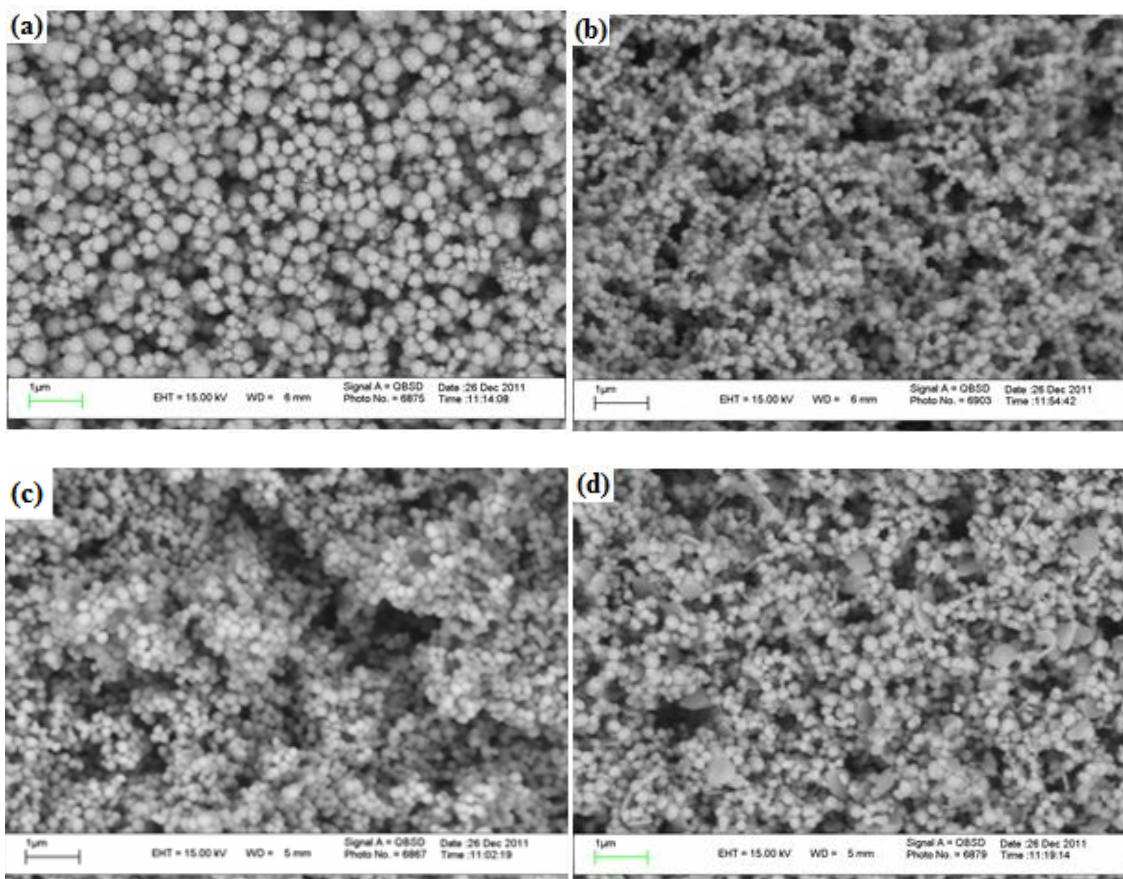


Fig. 1. (a, b, c, d) SEM images of Cu-Ag nanoparticles: (a) 10 at%, (c) 25 at%, (c) 50 at% and (d) 75 at%.

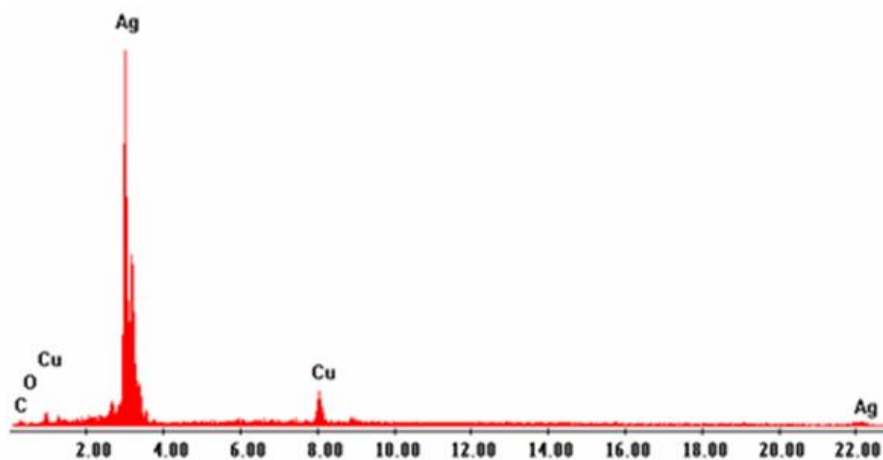


Fig. 2. EDAX Spectrum of the Cu-Ag nanoparticles: (a) 50 at%.

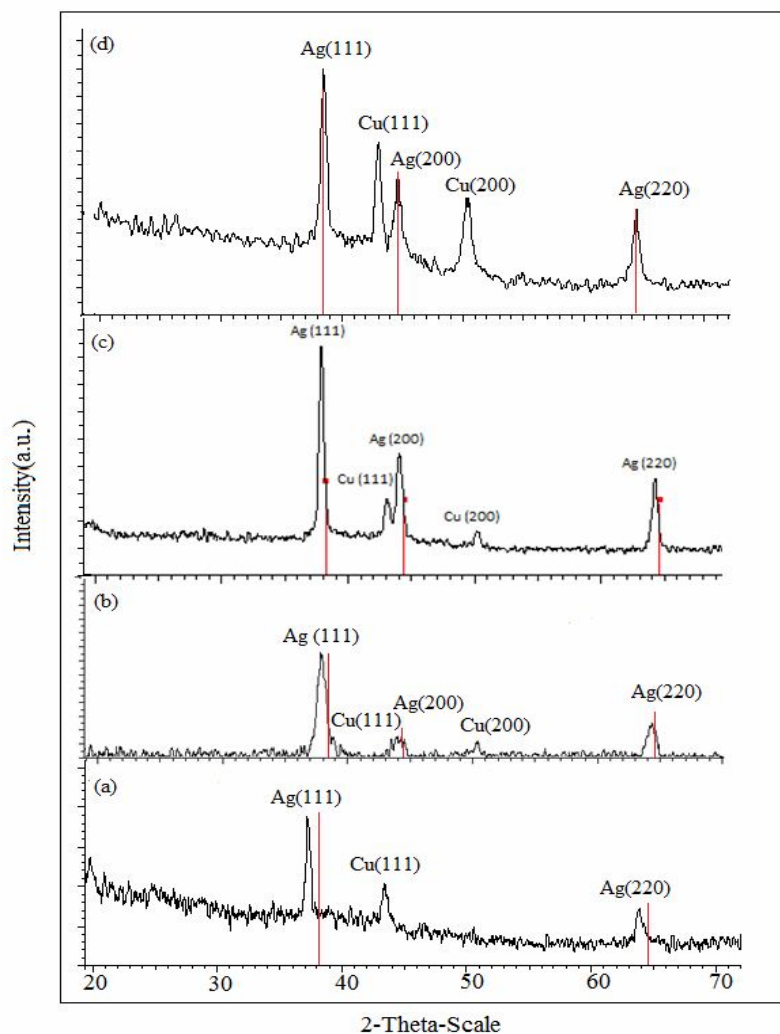


Fig. 3. X-ray diffraction patterns of the (a) 10% Cu, (b) 25% Cu, (c) 50% Cu and (d) 75% Cu.

Table 1. Detailed Experimental Parameters for Preparation of Ag-Cu Nanoparticles

Morphology	Concentration of $\text{CuSO}_4 \cdot 5\text{H}_2\text{O}$ (M)	Concentration of AgNO_3 (M)	Percentage of Cu (%)	Concentration of ascorbic acid (M)	Concentration of Anhydride maleic (M)	Sediment color
Spherical.Fig. 1a	0.00755	0.1	10%	0.04	0.001	Gray
Spherical.Fig. 1b	0.022	0.1	25%	0.04	0.001	Gray
Spherical.Fig. 1c	0.06	0.1	50%	0.04	0.001	Gray
Mixture of spherical and hexagonal.Fig. 1d	0.204	0.1	75%	0.04	0.001	Gray

The values of nano crystal for different percentages of copper are listed in Table 2, from which it is clear that the nano crystal decreases with the increase of Cu percentage.

Optical Study

UV-Vis absorption spectra of Ag-Cu nanoparticles, along with the pure sample of Ag, are shown in Fig. 4. The absorption peak of pure Ag is observed at about 410 nm. For Ag-Cu (10%, 25%, 50% Cu) only a single SPR absorption band is revealed, which corresponding peak position is different from that of the Ag nanoparticles. The UV-Vis spectrum shows absorption peaks at 380 nm (for 10% Cu), 370 nm (for 25% Cu), 350 nm (for 50% Cu). Nanoparticles of metals such as silver and copper in the size nano strongly scatter and adsorb light due to surface plasmon resonance (SPR). The frequency and intensity of SPR band depend on the size, shape, structure and composition [7,8] of the metal nanoparticles. As shown in this figure, the SPR peak position was blue-shifted with an increasing Cu percentage due to smaller particle sizes in the study. In these nanoparticles, the SPR frequency can be modulated in the range from SPR frequency of Ag

nanoparticles, by changing the percentages of Cu, and hence, is controlled, which is of great theoretical and practical importance.

Theoretical approach about plasmon resonance and particle size. There is some relationship between the absorption spectrum of silver or copper nanoparticles caused by surface plasmon absorption and their sizes. For nanoparticles, the excitation of the surface resonance absorption can occur in invisible light region. Such absorption spectra can be analyzed using Mie theory. In particular, according to this theory, for nanoparticles smaller than the mean free path of the conduction electrons there is a relationship between the resonance broadening (γ) and the sizes of nanoparticles

$$\gamma(R) = \gamma_0 + (A v_F) / R [9-12]$$

where r is the size of nanoparticles, A attached to scattering process ($A = 3/4$ for silver [13-14]), γ is the velocity of bulk scattering (for silver $5 \times 10^{12} \text{ S}^{-1}$) and v_F is the Fermi velocity (for silver $1.39 \times 10^6 \text{ m s}^{-1}$ [15-17]). Size depending of γ , leads to size depending of dielectric function $\epsilon(\omega, r)$ of

Table 2. Crystallite Size Variation with Different Percent of Copper from XRD Analysis

	Cu (10%)	Cu (25%)	Cu (50%)
Crystallite size (nm)	10.5	7.3	5.9

Table 3. Comparison FTIR Vibrational Assignments MA-Sample

FTIR Frequencies MA-Sample (cm ⁻¹)	Assignments
505.70	C-C out of plane
822.73	C-C ring
1319.79	CH ₂ wag
1363.79	CH bend
1652.69	C = O
2925.32	CH stretch
3405.09	OH stretch

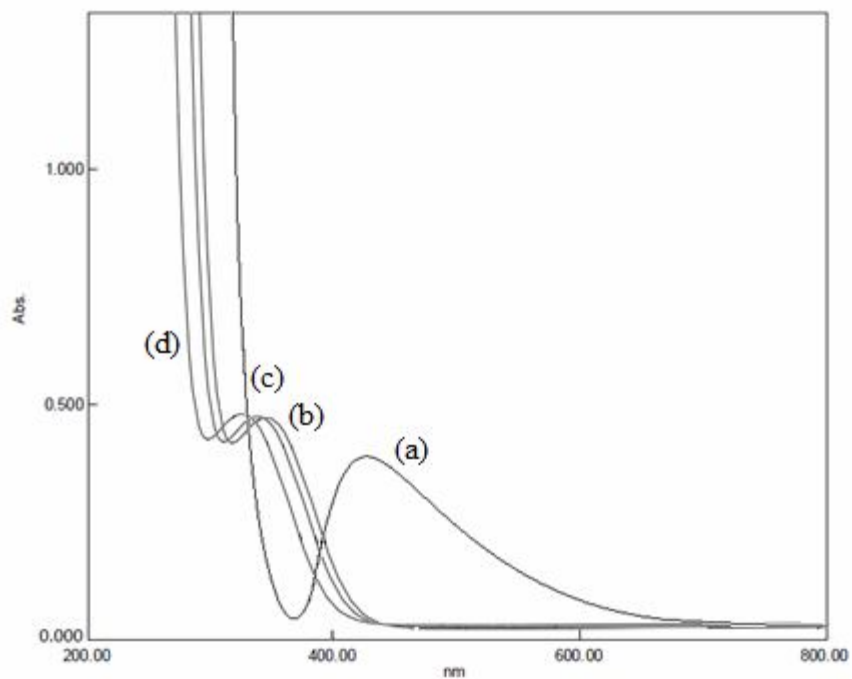


Fig. 4. Optical absorption spectrum of (a) Pure Ag, (b) 10% Cu, (c) 25% Cu and (d) 50% Cu.

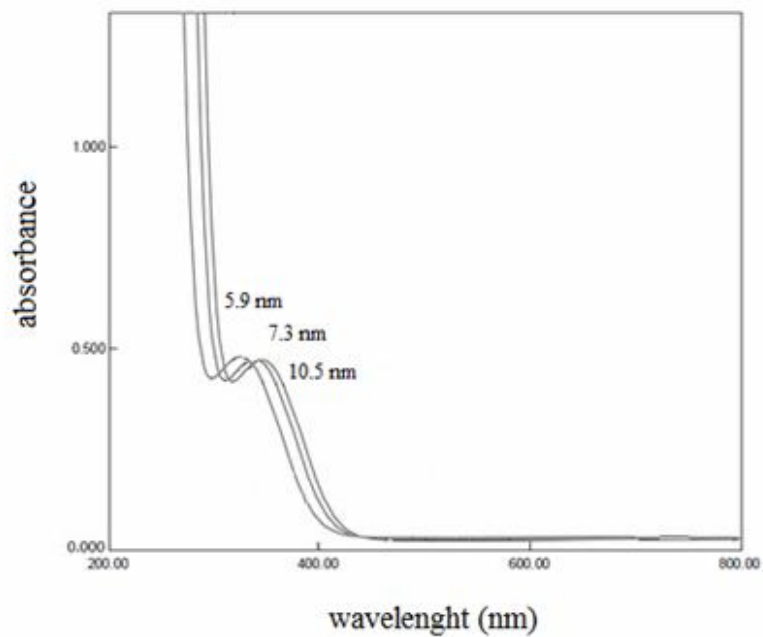


Fig. 5. Extinction spectra of Ag-Cu nanoparticles in different size. For this nanoparticles, the SPR wavelength is depending on the size of the nanoparticles.

metal and surrounding medium [18]. The actual part of the dielectric constant of the metal determines the SPR position and the imaginary part determines the bandwidth. The SPR resonance occurs when $\epsilon_r(\omega) = -2\epsilon_m$ [19]. Silver and copper nanoparticles show strong SPR bands in the visible region while other metals show broad and weak bands in the UV region [20]. Ag NPs show the SPR band around 410 nm in

the visible region. The SPR band is shifted by the particle size (Fig. 5). Decreasing particle size leads to the blue shifts in the SPR wavelength.

FTIR Analysis

FTIR spectroscopy was used to analyze the interaction between the metal and MA. Figure 6 shows the FTIR

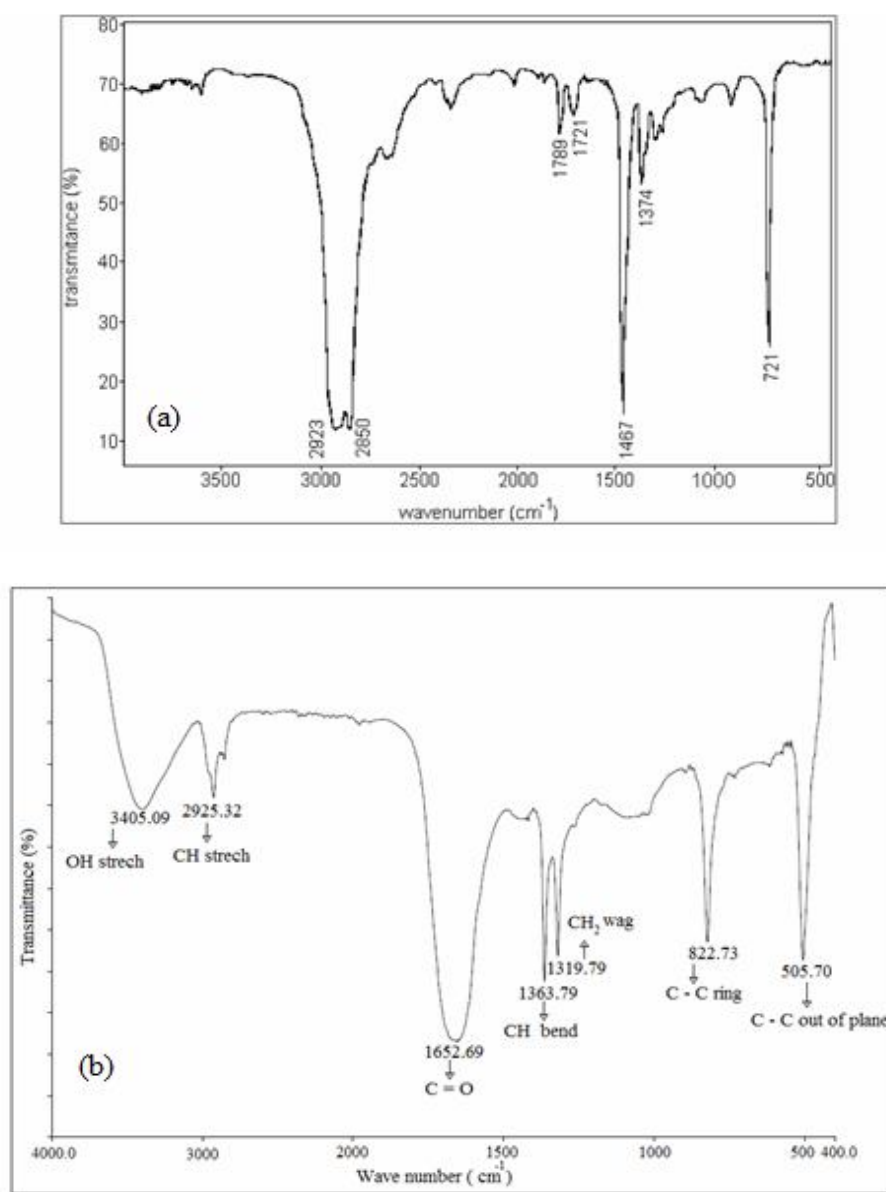


Fig. 6. FTIR spectra for the (a) pure MA [24] (b) MA-Sample (50% Cu).

spectrum for pure MA [21] and MA cladded nanoparticles (for 50% Cu). For MA the most characteristic anhydride bands C=O can be seen at 1860 and 1780 cm^{-1} (both peaks to the MA carbonyl groups). 1860 and 1780 cm^{-1} peaks are response from symmetric and asymmetric stretching of the MA carbonyl. The exact position of these bands is slightly dependent on the nature of the sample as well as the solvent used [22]. This peak was also confirmed by O-H stretching peak (3200-3300 cm^{-1}) because cyclic dimer has a center of symmetry. In the sample, the peak at 1780 cm^{-1} , representing the functional unit C=O present in MA, shifts to 1652.69 cm^{-1} after embedding nanoparticles. This change of the spectrum is indicative of the coordination between O atoms of C=O bands and nanoparticles.

CONCLUSIONS

In summary, Ag-Cu nanoparticles were synthesized through wet-chemical route. Scanning electron microscopy (SEM) indicated the formation of uniform spherical crystalline nanoparticles in a well distributed size and morphology for nanoparticles ($\leq 50\%$ Cu). When the molar ratio of $\text{Cu}^{2+}/\text{Ag}^+$ was 75/25 ($>50\%$ Cu), mixture of the spherical and hexagonal nanoparticles was prepared. The SPR peak position was blue-shifted with an increasing Cu percentage; therefore, by controlling the initial percentages of copper and silver in the reaction, we could control the SPR frequency of Ag-Cu nanoparticles.

ACKNOWLEDGMENTS

The authors express their thanks to the Research Vice Presidency of Science and Research Branch, Islamic Azad University and Iran Nanotechnology Initiative for their encouragement, and financial supports.

REFERENCES

- [1] Y. Ding, F. Fan, Z. Tian, Z. Wang, Atomic structure of Au-Pd bimetallic alloyed nanoparticles. *J. Am. Chem. Soc.* 132 (2010) 12480, DOI: 10.1021/ja105614q.
- [2] A. Ceylan, K. Astrzembki, S.I. Shah, Enhanced solubility Ag-Cu nanoparticles and their thermal transport properties. *J. Metallurg. Mater. Trans. A.* 37 (2006) 2033, DOI: 10.1007/BF02586123.
- [3] Y. Ma, M. Wei, X. Zhang, T. Zhao, X. Liu, G. Zhou, Spectra study of interaction between chondroitin sulfate and nanoparticles and its application in quantitative analysis. *J. Spectrochimica Acta Part A: Molecular and Biomolecular Spectroscopy.* 153 (2015) 445, DOI: 10.1016/j.saa.2015.08.045.
- [4] J.F. Sanchez-Ramirez, C. Vazquez-Lopez, U. Pal, Preparation and optical absorption of colloidal dispersion of Au/Cu nanoparticles. *J. Superficies y Vacio.* 15 (2002) 16.
- [5] C.D. Geddes, *Metal-Enhanced Fluorescence* (Ed.), Wiley, 2010, p. 574.
- [6] P. Mashayekhi, N. Farhadyar, Structural and optical behavior of Cu doped Au nanoparticles synthesized by wet-chemical method. *J. International Journal of Bio-Inorganic Hybrid Nanomaterials.* 2 (2013) 379.
- [7] C.F. Bohren, D.R. Huffman, *Absorption and Scattering of Light by Small Particles* (Ed.), Wiley, New York, 1998.
- [8] M.A. El-Sayed, Some interesting properties of metals confined in time and nanometer space of different shapes. *J. Accounts Chem. Res.* 34 (2001) 257, DOI: 10.1021/ar960016n.
- [9] A.O. Pinchuk, G.C. Schatz, Nanoparticle optical properties: Far- and near-field electrodynamic coupling in a chain of silver spherical nanoparticles, *J. Mater. Sci. Eng.* 149 (2008) 251, DOI: 10.1016/j.mseb.2007.09.078.
- [10] A. Pack, M. Hietschold, R. Wannemacher, Failure of local mie theory: optical spectra of colloidal aggregates. *J. Opt. Commun.* 194 (2001) 277, DOI: 10.1016.S0030-4018(01)01310-4.
- [11] M. Vollmer, U. Kreibig, *Nuclear Physics Concepts in the Study of Atomic Cluster Physics*, Springer Verlag, New York, USA, 1992.
- [12] I. Lisiecki, F. Billoudet, M.P. Pileni, Control of the shape and the size of copper metallic particles. *J. Phys. Chem.* 100 (1996) 4160, DOI: 10.1021/jp9523837.
- [13] U. Kreibig, C.Z. Fragstein, The limitation of electron mean free path in small silver particles. *J. Z. Phys.* 224 (1969) 307, DOI: 10.1007/BF01393059.

- [14] P. Apell, R. Monrea, F. Flores, Effective relaxation time in small spheres: diffuse surface scattering. *J. Solid State Commune.* 52 (1984) 971, DOI: 10.1016/0038-1098(84)90490-3.
- [15] S.N. Abdullin, A.L. Stepanov, Y.U. Osin, I.B. Khaibullin, Kinetics of silver nanoparticle formation in a viscous-flow polymer. *J. Surf. Sci.* 395 (1998) 242, DOI: 10.1016/S0039-6028(97)00849-2.
- [16] J. Singh, Effective mass of charge carriers in amorphous semiconductors and its applications. *J. Non-Cryst. Solids.* 299 (2002) 444, DOI: 10.1016/S0022-3093(01)00957-7.
- [17] N.W. Ashcroft, N.D. Mermin, *Solid State Physics*, International Thomson Publishing, 1976.
- [18] A. Henglein, P. Mulvaney, T. Linnert, Chemistry of Ag_n aggregates in aqueous solution: non-metallic oligomeric clusters and metallic particles. *J. Faraday Discuss.* 92 (1991) 31, DOI: 10.1039/FD9919200031.
- [19] X. Huang, M.A. El-sayed, Gold nanoparticles: Optical properties and implementations in cancer diagnosis and photothermal therapy. *J. Adv. Res.* 1 (2010) 13, DOI: 10.1016/j.jare.2010.02.002.
- [20] J.A. Creighton, D.G. Eadon, Ultraviolet-visible absorption spectra of the colloidal metallic elements. *J. Chem. Soc. Farad Trans.* 87 (1991) 3881, DOI: 10.1039/FT9918703881.
- [21] Y. Magdy, I. Abdelaal, H. Elsayed, Elmoosalamy, O.S. Saleh Bahaffi, Enhancement of polyolefins compatibility with natural fibers through chemical modification. *Am. J. Polymer Sci.* 2 (2012) 102, DOI: 10.5923/j.ajps.20120205.04.
- [22] B.C. Trivedi, B.M. Culbertson, *Maleic Anhydride*, New York and London, Plenum Press, New York and London, 1982.